The spliceosome inhibitors isoginkgetin and pladienolide B induce ATF3-dependent cell death

Erin J. Vanzyl[1] , Hadil Sayed[1] , Alex B. Blackmore[1], Kayleigh R.C. Rick[1], Pasan Fernando[1] and Bruce C. McKay[1,2*]

[1] Department of Biology, Carleton University, Ottawa, ON, Canada

[2]Institute of Biochemistry, Carleton University, Ottawa, ON, Canada

[*] Corresponding author

Email: bruce_mckay@carleton.ca

Abstract

The spliceosome assembles on pre-mRNA in a stepwise manner through five successive pre-spliceosome complexes. The spliceosome functions to remove introns from pre-mRNAs to generate mature mRNAs that encode functional proteins. Many small molecule inhibitors of the spliceosome have been identified and they are cytotoxic. However, little is known about genetic determinants of cell sensitivity. Activating transcription factor 3 (ATF3) is a transcription factor that can stimulate apoptotic cell death in response to a variety of cellular stresses. Here, we used a genetic approach to determine if ATF3 was important in determining the sensitivity of mouse embryonic fibroblasts (MEFs) to two splicing inhibitors: pladienolide B (PB) and isoginkgetin (IGG), that target different pre-spliceosome complexes. Both compounds led to increased ATF3 expression and apoptosis in control MEFs while ATF3 null cells were significantly protected from the cytotoxic effects of these drugs. Similarly, ATF3 was induced in response to IGG and PB in the two human tumour cell lines tested while knockdown of ATF3 protected cells from both drugs. Taken together, ATF3 appears to contribute to the cytotoxicity elicited by these spliceosome inhibitors in both murine and human cells.

Introduction

Most protein-coding genes are transcribed into a precursor RNA (pre-mRNA) that requires significant processing to produce mature mRNA. One of the more complex modifications is the removal of introns and ligation of exons through the process of pre-mRNA splicing [1]. The major spliceosome is responsible for the removal of the vast majority of introns, so it is usually referred to as the spliceosome[1]. The spliceosome is composed of five small nuclear RNAs (snRNAs), U1, U2, U4, U5 and U6, which are each associated with specific proteins yielding

41 their corresponding small nuclear ribonucleoprotein complexes (snRNP). These snRNPs bind
42 sequentially to *cis*-acting elements in pre-mRNA including the 5' and 3' splice sites, the branch
43 sequence, and polypyrimidine tract, leading to the assembly of a functional spliceosome through
44 the E, A, B, B* and C pre-spliceosome complexes [2].
45 A variety of small molecules interfere with the spliceosome at distinct points in assembly. PB is
46 a spliceosome inhibitor derived from *Streptomyces platensis* that targets the SF3B1 protein [3].
47 This protein is a component of the U2 snRNP complex so PB prevents the formation of the A
48 complex [3]. IGG is a natural compound derived from *Ginkgo biloba*, that affects the
49 spliceosome at a subsequent step, preventing the transition from the A to the B complex by
50 inhibiting the stable binding of the U4/U5/U6 tri-snRNP complex [[4]. These two compounds
51 affect different stages of spliceosome formation and it is unclear if they induce cytotoxicity
52 through one or more common pathways [5, 6].
53 Activating transcription factor 3 (ATF3) is a member of the ATF/CREB transcription factor
54 family and is activated in response to a variety of stresses including DNA damage, inflammation,
55 endoplasmic reticulum (ER) stress and oxidative stress [7-10]. ATF3 has been shown to have a
56 variety of functions, one of which is regulating the expression of proapoptotic genes, such as
57 GADD153/CHOP [11]. We sought to determine if ATF3 plays a role in determining the
58 sensitivity of mammalian cells to the inhibition of pre-mRNA splicing. Here we report that
59 ATF3 is induced in murine and human cells and that deletion of ATF3 in mouse embryonic
60 fibroblasts (MEFs) and knockdown of ATF3 in HeLa cells protects them from the lethal effects
61 of spliceosome inhibitors. This work provides important insight into the genetic basis of cell
62 death induced by spliceosome dysfunction.
63

64 **Materials and Methods**

65 *Cell culture and drug treatment*

66 ATF3$^{+/+}$ and ATF3$^{-/-}$ MEFs were obtained from Dr. Jim Dimitroulakos (Ottawa Hospital
67 Research Institute)[12] and grown in DMEM High Glucose media (Hyclone, San Angelo)
68 supplemented with 10% fetal calf serum (FBS) (Gibco, ThermoFisher Scientific, Ottawa) and 90
69 units/ml penicillin, 90 ug/ml streptomycin (Hyclone). HCT116 and HeLa cells were obtained
70 from the American Tissue Type Collection (Cat #: CCL-247 and CCL-2,, Manassas, VA) grown
71 in McCoys and DMEM media (Hyclone), respectively, supplemented with a 3:1 mixture of
72 Newborn Calf Serum (NBCS) (Gibco, Thermo Fisher Scientific) and Fetal Calf Serum (FBS)
73 (Gibco, ThermoFisher Scientific), and 90 units/ml penicillin, 90 ug/ml streptomycin (Hyclone).
74 Cell were seeded at a density of 500,000 cells/6 cm or 25,000 cells per well of a 96-well plate, 24
75 hours prior to treatment, depending on the assay. Cells were treated with up to 30 µM IGG
76 (Calbiochem), up to 25nM PB (ChemCruz), 200nM actinomycin D (act D) (Sigma-Aldrich, St.
77 Louis, MO), an equivalent volume of dimethyl sulfoxide (DMSO) as the vehicle control for IGG
78 or left untreated.

79

80 *Reverse transcription (RT) and real time quantitative polymerase chain reaction (RT-qPCR)*

81 RNA was isolated using the EZ-10 DNAaway RNA Miniprep Kit (Biobasics, Markham ON) and
82 quantified using a DeNovix DS-11 Spectrophotometer (Wilmington, DE). Equal amounts of
83 RNA were converted to cDNA using the High Capacity cDNA Reverse Transcription kit
84 (ThermoFisher Scientific). For MEF experiments, ATF3 mRNA expression was determined
85 using Bioline SensiFAST™ Probe HI-ROX Master Mix (FroggaBio Inc, Toronto, ON) with

86 SYBR green. ATF3 expression was normalized to the average of two housekeeping genes; β-
87 actin (ACTB) and Peptidylprolyl isomerase A (PPIA) using the following primers: ATF3 (F-
88 AAGACAGAGTGCCTGCAGAA, R-GTGCCACCTCTGCTTAGCTC), ACTB (F-
89 GATCTGGCACCACACCTTCT, R-GGGGTGTTGAAGGTCTCAAA) and PPIA (F-
90 AGCTCTGAGCACTGGAGAGA, R-GCCAGGACCTGTATGCTTTA). Primers were
91 synthesized by Integrated DNA Technologies (Coralville, Ia). For human samples, ATF3 mRNA
92 expression was measured using the Hs00231069_m1 TaqMan® Gene Expression Assays
93 (ThermoFisher Scientific) with GAPDH serving as a sample control (Hs02758991_g1).

94 *Immunoblotting*

95 Cell monolayers were rinsed with phosphate buffered saline (PBS) pH 7.6 and collected in 300µl
96 of 1% SDS. Samples were sonicated (QSonic, Newton), and protein was quantified using the
97 Bio-Rad Protein Assay (Bio-Rad, Philadelphia). Equal amounts of protein were denatured in
98 NuPAGE™ LDS Sample Buffer and NuPAGE™ Sample Reducing Agent (10X) (ThermoFisher
99 Scientific, Ottawa), heated for 10 minutes at 70°C and loaded onto NuPAGE 4-12% Bis-Tris
100 gels (Fisher Scientific). Protein was then transferred to a nitrocellulose membrane (Bio-Rad), and
101 transferred proteins were stained using 1mg/ml Ponceau S Red in 1% glacial acetic acid.
102 Membranes were blocked for 30-60 minutes in 5% Milk in Tris Buffered Saline Tween (TBST)
103 pH 7.6 (Tris Buffered Saline, 0.1% Tween 20). Membranes were incubated overnight at 4°C in
104 primary antibody, anti-ATF-3 (sc-188, Santa Cruz, CA) or anti-beta-actin (A2228, Sigma)
105 diluted 1:200 for ATF3 or 1:1000 for Actin in 0.5% Milk in TBST pH 7.6. Membranes were
106 washed 4×5 min in TBST, then incubated in secondary antibody (HRP-conjugated goat anti-
107 mouse or goat anti-rabbit from Abcam) for 1-2 hours. Membranes were washed 4×5 min in

108 TBST, then incubated for 5 minutes in 600µl of Clarity™ Western ECL substrate (Bio-Rad), and
109 imaged using the Fusion FX5 gel documentation system (Vilber Lourmat, France).

110 *Flow cytometry*

111 Floating and adherent cells were collected and combined 48 hours following treatment by
112 centrifugation following trypsin treatment. The supernatant was removed, and the cell pellet was
113 washed twice in PBS, fixed in 1ml ice cold 70% ethanol, and stored at −20°C for a minimum of
114 30 minutes. Cells were centrifuged, ethanol was then removed, and the pellet was washed twice
115 in PBS and resuspended in 200µl of 20µM Propidium Iodide (PI) stain (Sigma-Aldrich) with
116 73µM RNaseA (Fisher Scientific). Red fluorescence was measured with a BD Accuri C6 flow
117 cytometer and analyzed using the BD Accuri C6 software.

118 *Cell viability assays*

119 $ATF3^{+/+}$ and $ATF3^{-/-}$ MEFs were seeded in a 96-well plate 24h hours prior to treatment for both
120 cell viability assays. The trypan blue dye exclusion assay was used as an early indicator of cell
121 death detected at 24 hours, prior to cell detachment. For trypan blue dye exclusion assays, cells
122 were detached using trypsin 24 hours after treatment. Ten ul of trypan blue (0.4% in PBS) was
123 added to each well of the 96-well plate. After two minutes, an aliquot of cells was transferred to
124 Dual-Chamber cell counting slides (Bio-Rad, Hercules) and read using the Biorad TC20
125 Automated Cell Counter.

126

127 A luminescent ATP based cell viability assay was used as an indicator of a later stage of cell
128 death after significant cell detachment was detected (48 hours). The CellTiter-Glo® Luminescent
129 Cell Viability Assay (Promega, Madison) was used according to manufacturer's instructions to

130 determine ATP content, to estimate cell viability. Briefly, 100 µl of media was removed from
131 each well and mixed with an equal volume of CellTiter-Glo Reagent. After 2 minutes of shaking,
132 the samples were incubated at room temperature for 10 minutes and read using the Cytation 5 96
133 well plate reader (BioTek, Vermont) and Gen5 software (version 2.07.17) at an integration time
134 of 1.0 s per well.
135
136 *siRNA-mediated knockdown of ATF3*
137 SMARTpool ON-TARGETplus siRNA (cat#: L-008663-00- 0005 and D-001810-10-05,
138 Dharmacon Inc, Chicago) were prepared in siRNA buffer as recommended by the manufacturer.
139 HeLa cells were seeded at $2x10^6$ cells per 10 cm dish, in antibiotic free growth media 24 hours
140 prior to transfection. The siRNAs were combined with lipofectamine 3000 as recommended by
141 the manufacturer (ThermoFisher Scientific) to a final concentration of 50 nM in antibiotic and
142 serum free media. The siRNAs were added to cells for 48 hours, after which transfected cells
143 were seeded at $5x10^5$ cells per 6 cm dish for mRNA and protein collection and $1.25x10^5$ in 6 well
144 dishes for flow cytometric analysis. Cell were treated 24 hours later and samples were collected
145 at the indicated times for RNA, protein, and apoptosis assays from the same siRNA transfection.
146
147 **Results**

148 *ATF3 is induced and contributes to cell sensitivity in mouse embryonic fibroblasts*

149 Pre-mRNA splicing is essential for viability and pre-mRNA splicing inhibitors are cytotoxic
150 through an unknown mechanism. It was recently reported that IGG-induces ATF3 indirectly
151 through ATF4, however it was unclear if ATF3 contributed to cell death [13]. Therefore, we
152 used a simple genetic approach to determine if ATF3 contributes to cell death following

153 spliceosome inhibition using isogenic MEF strains that either expressed or did not express ATF3
154 (ATF3$^{+/+}$ and ATF3$^{-/-}$ MEFs, respectively). ATF3 mRNA levels increased significantly in the
155 ATF3$^{+/+}$ MEFs in response to PB but not IGG exposure (Fig 1A). ATF3 protein increased in
156 response to both drugs, however we detected a greater increase in response to PB (Fig 1B). As
157 expected, ATF3 protein was not detected in the ATF3$^{-/-}$ MEFs (Figure 1B). We then assessed
158 sensitivity to apoptosis by one parameter flow cytometric analysis of sub G_1 DNA content in
159 both cell lines following exposure to IGG and PB (Fig. 1B). Both drugs led to an increase in the
160 proportion of cells with less than diploid DNA content, however PB led to a greater increase than
161 IGG (Fig 1C). Importantly, cells deleted of ATF3 were significantly protected from drug-
162 induced apoptosis compared to isogenic controls following exposure to both drugs. Therefore,
163 ATF3 appears to contribute to PB- and IGG- induced apoptosis in MEFs.
164
165 The sensitivity of MEFs to spliceosome inhibition was further evaluated with two additional
166 independent assays. First, ATF3$^{+/+}$ and ATF3$^{-/-}$ MEFs were exposed to either IGG or PB for 24h
167 and cell viability was assessed by trypan blue dye exclusion (Fig 2A). Trypan blue is unable to
168 penetrate viable cells with intact cell membranes, whereas non-viable cells that have lost
169 membrane integrity take up the dye. Both splicing inhibitors (PB and IGG) decreased cell
170 viability in ATF3$^{+/+}$ MEFs. The surviving fractions of ATF3$^{-/-}$ MEFs were significantly higher
171 than parental controls following exposure to both drugs. In fact, there was no detectable decrease
172 in viability in the ATF3$^{-/-}$ MEFs with this assay.
173
174 Second, a CellTiter-Glo® Luminescent Cell Viability Assay was used to quantify ATP levels in
175 treated and untreated cells. A decrease in ATP in treated compared to untreated cells is indicative

176 of a decrease in the number of metabolically active cells (Fig 2B). ATP levels decreased in both
177 $ATF3^{+/+}$ and $ATF3^{-/-}$ MEFs following treatment with IGG and PB, however the surviving
178 fraction of treated $ATF3^{-/-}$ MEFs was significantly greater than the surviving fraction of control
179 MEFs. $ATF3^{-/-}$ MEFs were again protected from the cytotoxic effects of both PB and IGG.
180 Taken together, ATF3 expressing MEFs are more sensitive to splicing inhibitors than their
181 $ATF3^{-/-}$ counterparts, as assessed by DNA fragmentation, membrane integrity and ATP content.
182 ATF3 is important in multiple cell death pathways [7, 11, 14] but its contribution to cell
183 sensitivity to the spliceosome inhibitors was unknown.
184
185 *Splicing inhibitors increase ATF3 expression in human cells*
186 Our results provide compelling genetic evidence that ATF3 contributes to cell death induced by
187 spliceosome inhibitors in MEFs. We sought to determine if splicing inhibitors similarly led to
188 ATF3 induction in human cells. Therefore, we measured the expression of ATF3 mRNA and
189 protein in response to treatment with both splicing inhibitors in colorectal carcinoma and cervical
190 carcinoma cells (HCT116 and HeLa cells, respectively). As detected in MEFs, ATF3 mRNA
191 increased significantly in response to PB in both cell lines while the small increase in ATF3
192 mRNA in IGG treated cells was not statistically significant (Fig. 3A and B). Again, ATF3
193 protein was induced more in response to PB than IGG (Fig. 3C and D). Both cancer cell lines
194 were exposed to either IGG or PB and 48 hours later apoptosis was assessed by flow cytometric
195 analysis of subG1 DNA content. Both splicing inhibitors resulted in an increase in the fraction of
196 cells with sub G1 DNA content under the same conditions with higher levels of apoptosis
197 detected in response to PB (Figs 3 E and F), consistent with greater fold increases in ATF3

198 expression. These results support the concept that ATF3 is induced upon spliceosome disruption
199 and that this could contribute to cell death in human cells as well.
200

201 *Knockdown of ATF3 protects HeLa cells from spliceosome inhibitors*

202 To determine if ATF3 contributes to cell sensitivity in response to splicing inhibitors in these
203 human cancer cell lines, we performed siRNA mediated knockdown of ATF3 in HeLa cells. The
204 siRNA transfected cells were seeded to smaller dishes to perform all assays from the same
205 transfected sample. RNA interference led to decreased ATF3 expression and prevented the full
206 induction of ATF3 following drug exposure (Figs 4A and B). As expected, ATF3 knockdown
207 protected HeLa cells against the cytotoxic effects of these splicing inhibitors, although only
208 protection against PB was statistically significant (Fig 4C). These results support the concept that
209 ATF3 is induced upon spliceosome disruption and that this contributes to cell death in both
210 murine and human cells.
211

212 **Discussion**

213 The production of functional mRNAs requires the synthesis of pre-mRNA that is coordinated
214 with co-transcriptional mRNA processing steps including pre-mRNA splicing [15-17]. The
215 inhibition of pre-mRNA splicing delays or prevents the production of functional mRNAs and
216 indirectly the encoded proteins. How splicing abnormalities are sensed and transmitted to cell
217 death pathways remains unclear. In the present work, we measured cellular responses to two
218 spliceosome inhibitors, IGG and PB. We found that both drugs led to an increase in ATF3
219 expression in human colon cancer cells and MEFs. Parental MEFs, expressing ATF3, were
220 sensitive to both inhibitors leading to a large decrease in the viable cell population. However,

221 cell viability was significantly higher in ATF3-/-, as assessed in 3 independent assays. Subtle
222 quantitative differences were detected among the assays that reflect the timing of individual
223 assays, the measured characteristic of cell death (DNA fragmentation, loss of membrane integrity
224 or loss of ATP) and the sensitivity of individual assays. In addition, CellTiter-Glo® Luminescent
225 Cell Viability Assay is not determined on a single cell basis and it is very sensitive [18] so it isn't
226 entirely surprising that we detected greater apparent cell death with this assay. Despite these
227 differences, all three assays support a model in which ATF3 is a major regulator of mammalian
228 cell sensitivity to these pre-mRNA splicing inhibitors.
229
230 To address the importance of ATF3 in determining the sensitivity of human cells to spliceosome
231 inhibitors, we used siRNAs to target ATF3 in HeLa cells. We were able to knockdown ATF3 by
232 about 50% prior to treatment and RNA interference prevented the induction of ATF3 by IGG
233 and PB. Consistent with data obtained in MEFs, we found that reduced ATF3 expression was
234 associated with decreased sensitivity to apoptosis. Therefore, ATF3 appears to contribute to
235 IGG- and PB-induced cell death in human cells, as well. It is noteworthy that PB led to higher
236 ATF3 levels and greater sensitivity to cell death in all cell lines, consistent with ATF3-dependent
237 apoptosis. This is remarkable in that the concentrations of PB used here are well below the
238 reported IC50 for inhibition of *in vitro* splicing (90 nM) while there is less ATF3 and cell death
239 induced by IGG at its reported in vitro IC50 (30 μM) [4, 19]. It is unclear why we detected
240 differences in ATF3-dependent apoptosis but this adds to a growing list of differences reported
241 in the literature.
242

243 The two spliceosome inhibitors tested target distinct pre-spliceosome complexes. PB interacts
244 with the SF3B1 subunit of the U2 snRNP in the complex A [5] whereas IGG acts somewhat later
245 preventing the transition from the A to B complex through an unknown target [4]. Even though
246 both drugs inhibit pre-mRNA splicing at similar stages and induce apoptosis through an ATF3-
247 dependent mechanism, a variety of differences in gene expression and biological effects have
248 been described. For example, we have previously reported that these two drugs can have
249 pronounced effects on cell cycle distribution but these changes were not identical [20]. Two
250 parameter flow cytometric analysis of bromodeoxyuridine-labelled cells indicated that IGG led
251 to multiple cell cycle alterations but the most prominent was to an S phase arrest [20]. In partial
252 contrast, PB-treated cells were blocked predominantly in G_1 but also exhibited a more modest S
253 phase arrest than IGG-treated cells [20]. Meanwhile, both drugs led to decreased M phase
254 assessed by loss of phospho-H3 immunoreactivity [20]. Therefore, there are similarities and
255 differences in the effects of these compounds on cell cycle responses.
256
257 Other groups have reported recently that IGG has other unique effects on transcription and
258 protein trafficking. Boswell and coworkers found that IGG decreases transcription elongation, in
259 addition to its effects on pre-mRNA splicing [21]. Strand-specific RNA-sequencing (RNA-seq)
260 was performed in IGG-treated and control cells and relative read number increased within 5 kb
261 of transcription start sites in IGG-treated cells but not in the presence of an SF3B1 inhibitor,
262 meayamycin [22], suggesting that transcription near the 5'end of genes was slow in the presence
263 of IGG [21]. These authors also detected increased polyA site readthrough in IGG treated cells
264 further suggesting that a fundamental problem in transcription and co-transcriptional processing
265 may underlie some of the unique biological effects of IGG [21]. It is noteworthy that these

266 authors still detected a defect in pre-mRNA splicing using RNA-seq analysis in this and previous
267 papers [21, 23, 24]
268
269 Lastly, IGG also appeared to inhibit trafficking of the amyloid precursor protein (APP) from
270 endoplasmic reticulum (ER) to the Golgi [24]and lysosome-mediated turnover [13]. In the
271 former, APP levels increased in response to IGG but not the SF3B1 inhibitor spliceostatin [24].
272 APP was retained in the ER where the protein was stable and accumulated [24]. In the latter
273 paper [13], IGG led to increased lysosomal stress, increased TFEB protein expression (a
274 regulator of lysosomal biogenesis) and the accumulation of polyubiquitinated proteins under
275 nutrient starving conditions suggesting that IGG may be inhibiting proteasomes and altering
276 lysosomal function under some conditions [13]. Intriguingly, IGG-induced TFEB activated
277 ATF3 indirectly through ATF4, however it was unclear if ATF3 contributed to cell death
278 detected in this manuscript. There is presently no evidence that PB or any other SF3B1 inhibitors
279 similarly affect protein homeostasis. While these additional functions attributed to IGG may
280 contribute to differences detected in cell cycle regulation [20], they don't appear to strictly alter
281 the ATF3-dependence of cell death induced by IGG and PB. It is likely that IGG and PB lead to
282 ATF3 induction through a common mechanism related to spliceosome inhibition.
283
284 **Conclusions**
285 ATF3 is involved in a variety of stress pathways, and it is likely that a disruption in spliceosome
286 formation is leading to activation of ATF3 through an unknown mechanism. The novel findings
287 here provide evidence that splicing inhibitors lead to activation of ATF3, and that ATF3, in turn,
288 is playing a role in determining sensitivity of cells to these compounds. Our future work will

289 investigate the role ATF3 has on cell sensitivity, and work to determine how each of these

290 splicing inhibitors specifically led to ATF3 activation.

291

292 **Acknowledgements**

293 We would like to thank Dr. Jim Dimitroulakos (Princess Margaret Research Institute, Toronto,

294 ON) for providing mouse embryonic fibroblasts.

295

296 **References**

297 1. Hoskins AA, Rodgers ML, Friedman LJ, Gelles J, Moore MJ. Single molecule analysis reveals
298 reversible and irreversible steps during spliceosome activation. Elife. 2016;5. doi: 10.7554/eLife.14166.
299 PubMed PMID: 27244240; PubMed Central PMCID: PMCPMC4922858.
300 2. Jurica MS, Moore MJ. Pre-mRNA splicing: awash in a sea of proteins. Molecular cell.
301 2003;12(1):5-14. doi: 10.1016/s1097-2765(03)00270-3. PubMed PMID: 12887888.
302 3. Kotake Y, Sagane K, Owa T, Mimori-Kiyosue Y, Shimizu H, Uesugi M, et al. Splicing factor SF3b as
303 a target of the antitumor natural product pladienolide. Nature chemical biology. 2007;3(9):570-5.
304 PubMed PMID: 17643112.
305 4. O'Brien K, Matlin AJ, Lowell AM, Moore MJ. The biflavonoid isoginkgetin is a general inhibitor of
306 Pre-mRNA splicing. The Journal of biological chemistry. 2008;283(48):33147-54. PubMed PMID:
307 18826947.
308 5. Yokoi A, Kotake Y, Takahashi K, Kadowaki T, Matsumoto Y, Minoshima Y, et al. Biological
309 validation that SF3b is a target of the antitumor macrolide pladienolide. FEBS J. 2011;278(24):4870-80.
310 doi: 10.1111/j.1742-4658.2011.08387.x. PubMed PMID: 21981285.
311 6. Yoon SO, Shin S, Lee HJ, Chun HK, Chung AS. Isoginkgetin inhibits tumor cell invasion by
312 regulating phosphatidylinositol 3-kinase/Akt-dependent matrix metalloproteinase-9 expression.
313 Molecular cancer therapeutics. 2006;5(11):2666-75. PubMed PMID: 17121913.
314 7. Fan F, Jin S, Amundson SA, Tong T, Fan W, Zhao H, et al. ATF3 induction following DNA damage
315 is regulated by distinct signaling pathways and over-expression of ATF3 protein suppresses cells growth.
316 Oncogene. 2002;21(49):7488-96. doi: 10.1038/sj.onc.1205896. PubMed PMID: 12386811.
317 8. Gurzov EN, Barthson J, Marhfour I, Ortis F, Naamane N, Igoillo-Esteve M, et al. Pancreatic beta-
318 cells activate a JunB/ATF3-dependent survival pathway during inflammation. Oncogene.
319 2012;31(13):1723-32. doi: 10.1038/onc.2011.353. PubMed PMID: 21841823.
320 9. Schroder M, Kaufman RJ. ER stress and the unfolded protein response. Mutation research.
321 2005;569(1-2):29-63. doi: 10.1016/j.mrfmmm.2004.06.056. PubMed PMID: 15603751.
322 10. Fels DR, Koumenis C. The PERK/eIF2alpha/ATF4 module of the UPR in hypoxia resistance and
323 tumor growth. Cancer Biol Ther. 2006;5(7):723-8. doi: 10.4161/cbt.5.7.2967. PubMed PMID: 16861899.
324 11. Thompson MR, Xu D, Williams BR. ATF3 transcription factor and its emerging roles in immunity
325 and cancer. J Mol Med (Berl). 2009;87(11):1053-60. doi: 10.1007/s00109-009-0520-x. PubMed PMID:
326 19705082; PubMed Central PMCID: PMCPMC2783469.

327 12. St Germain C, O'Brien A, Dimitroulakos J. Activating Transcription Factor 3 regulates in part the
328 enhanced tumour cell cytotoxicity of the histone deacetylase inhibitor M344 and cisplatin in
329 combination. Cancer Cell Int. 2010;10:32. doi: 10.1186/1475-2867-10-32. PubMed PMID: 20828393;
330 PubMed Central PMCID: PMCPMC2945341.
331 13. Tsalikis J, Abdel-Nour M, Farahvash A, Sorbara MT, Poon S, Philpott DJ, et al. Isoginkgetin, a
332 Natural Biflavonoid Proteasome Inhibitor, Sensitizes Cancer Cells to Apoptosis via Disruption of
333 Lysosomal Homeostasis and Impaired Protein Clearance. Molecular and cellular biology. 2019;39(10).
334 doi: 10.1128/MCB.00489-18. PubMed PMID: 30910794; PubMed Central PMCID: PMCPMC6497994.
335 14. Mungrue IN, Pagnon J, Kohannim O, Gargalovic PS, Lusis AJ. CHAC1/MGC4504 is a novel
336 proapoptotic component of the unfolded protein response, downstream of the ATF4-ATF3-CHOP
337 cascade. J Immunol. 2009;182(1):466-76. PubMed PMID: 19109178; PubMed Central PMCID:
338 PMCPMC2846782.
339 15. Saldivar JS, Wu X, Follen M, Gershenson D. Nucleotide excision repair pathway review I:
340 implications in ovarian cancer and platinum sensitivity. Gynecol Oncol. 2007;107(1 Suppl 1):S56-71.
341 Epub 2007/09/22. doi: S0090-8258(07)00518-5 [pii]

342 10.1016/j.ygyno.2007.07.043. PubMed PMID: 17884153.
343 16. Carmo-Fonseca M, Kirchhausen T. The timing of pre-mRNA splicing visualized in real-time.
344 Nucleus. 2014;5(1):11-4. doi: 10.4161/nucl.28056. PubMed PMID: 24637398; PubMed Central PMCID:
345 PMCPMC4028348.
346 17. Lee KM, Tarn WY. Coupling pre-mRNA processing to transcription on the RNA factory assembly
347 line. RNA Biol. 2013;10(3):380-90. doi: 10.4161/rna.23697. PubMed PMID: 23392244; PubMed Central
348 PMCID: PMCPMC3672281.
349 18. Nowak E, Kammerer S, Kupper JH. ATP-based cell viability assay is superior to trypan blue
350 exclusion and XTT assay in measuring cytotoxicity of anticancer drugs Taxol and Imatinib, and
351 proteasome inhibitor MG-132 on human hepatoma cell line HepG2. Clin Hemorheol Microcirc.
352 2018;69(1-2):327-36. doi: 10.3233/CH-189120. PubMed PMID: 29630545.
353 19. Effenberger KA, Anderson DD, Bray WM, Prichard BE, Ma N, Adams MS, et al. Coherence
354 between cellular responses and in vitro splicing inhibition for the anti-tumor drug pladienolide B and its
355 analogs. The Journal of biological chemistry. 2014;289(4):1938-47. doi: 10.1074/jbc.M113.515536.
356 PubMed PMID: 24302718; PubMed Central PMCID: PMCPMC3900944.
357 20. Vanzyl EJ, Rick KRC, Blackmore AB, MacFarlane EM, McKay BC. Flow cytometric analysis
358 identifies changes in S and M phases as novel cell cycle alterations induced by the splicing inhibitor
359 isoginkgetin. PLoS One. 2018;13(1):e0191178. doi: 10.1371/journal.pone.0191178. PubMed PMID:
360 29338026; PubMed Central PMCID: PMCPMC5770052.
361 21. Boswell SA, Snavely A, Landry HM, Churchman LS, Gray JM, Springer M. Total RNA-seq to
362 identify pharmacological effects on specific stages of mRNA synthesis. Nature chemical biology.
363 2017;13(5):501-7. doi: 10.1038/nchembio.2317. PubMed PMID: 28263964.
364 22. Albert BJ, McPherson PA, O'Brien K, Czaicki NL, Destefino V, Osman S, et al. Meayamycin inhibits
365 pre-messenger RNA splicing and exhibits picomolar activity against multidrug-resistant cells. Molecular
366 cancer therapeutics. 2009;8(8):2308-18. PubMed PMID: 19671752.
367 23. Gray JM, Harmin DA, Boswell SA, Cloonan N, Mullen TE, Ling JJ, et al. SnapShot-Seq: a method
368 for extracting genome-wide, in vivo mRNA dynamics from a single total RNA sample. PLoS One.
369 2014;9(2):e89673. doi: 10.1371/journal.pone.0089673. PubMed PMID: 24586954; PubMed Central
370 PMCID: PMCPMC3935918.
371 24. Bai B, Wang S, Chen Y, Jia J, Tian X, Liu C, et al. Effects of RNA Splicing Inhibitors on Amyloid
372 Precursor Protein Expression. ACS Omega. 2018;3(3):2798-803. doi: 10.1021/acsomega.7b02073.
373 PubMed PMID: 30221221; PubMed Central PMCID: PMCPMC6130791.

374 **Figure Legends**

375

376 **Fig 1. ATF3 is activated in response to IGG and PB treatment in MEFs.** ATF3$^{+/+}$ and ATF3^{-}
377 $^{/-}$ MEFs were left untreated, or exposed to DMSO, 30µM IGG or 25nM PB for 24 hours and
378 RNA and protein were collected (A and B). (A) ATF3 mRNA levels were quantified in 3
379 independent experiments in control MEFs using qRT-PCR, and statistical analysis was
380 performed using a one-way ANOVA followed by Tukey's post test. (B) Immunoblot analysis
381 was performed with the indicated antibodies. Similar results were obtained in 4 independent
382 experiments and the mean fold change is indicated below the blot. (C) Flow cytometric analysis
383 of sub G_1 content was performed 48 hours following treatment of ATF3$^{+/+}$ and ATF3$^{-/-}$ MEFs.
384 Each value represents the mean, +/- SEM, of at least 3 independent experiments. The '*' and
385 '**' indicate that the value is significantly different from that of its ATF3 expressing control
386 ($p<0.05$ and $p<0.01$, respectively) by unpaired t-test.

387

388 **Fig 2. The absence of ATF3 in MEFs increases cell viability following PB and IGG**
389 **treatment**. ATF3$^{+/+}$ MEFs (white) and ATF3$^{-/-}$ MEFs (grey) were incubated with 30µM IGG,
390 25nM PB and 200nM act D for 24h (A) or 48h (B). L and H refer different volumes of DMSO
391 required to serve as vehicle controls for the 2 concentrations of IGG. (A) A trypan blue exclusion
392 assay was used to assess membrane integrity, as an indicator of cell viability. (B) The CellTiter-
393 Glo® Luminescent Cell Viability Assay was used to estimate metabolic activity as an indicator
394 of cell viability. Each bar represents the mean of 3 independent experiments, +/- SEM. Statistical
395 significance between cell lines for each treatment was completed using a t-test (*$p<0.05$,
396 **$p<0.01$, ***$p<0.001$).

397

398 **Fig 3. ATF3 expression is increased in human cells exposed to IGG and PB.** HCT116 and
399 HeLa cells were left untreated, exposed to DMSO, 30μM IGG or 25nM PB for 24h (A-D) or 48
400 hours (E and F). (A-D) ATF3 mRNA and protein levels were measured using qRT-PCR and
401 immunoblotting, respectively, in HCT116 and HeLa cells. The mean fold change determined
402 from 3 independent experiments is presented below the representative lane of the immunoblot.
403 (E and F) Flow cytometric analysis of sub G_1 DNA content was performed 48 hours following
404 treatment of HCT116 and HeLa cells in response to IGG and PG, as indicated in each panel.
405 Each point represented the mean, +/- SEM from at least three independent experiments.
406 Statistical significance was determined using a one-way ANOVA followed by a Tukey's post-
407 test (*$p<0.05$).
408
409 **Fig 4. Knockdown of ATF3 protects HeLa cells from IGG- and PB-induced apoptosis.**
410 HeLa cells were transfected with control non-targeting or anti-ATF3 siRNAs, split into separate
411 dishes for RNA, protein, and apoptosis analysis. Transfected cells were subsequently exposed to
412 the indicated drugs (30 μM IGG or 25 nM PB), no drug control (ND) or vehicle control (DMSO)
413 for up to 48 hours. (A and B) Twenty-four hours following treatment, protein and RNA samples
414 were collected for immunoblot (A) and qRT-PCR analysis (B). Similar immunoblot results were
415 obtained over from three independent experiments. Each value in B represents the mean +/- SEM
416 determined from three independent experiments. (C) Sensitivity to IGG- and PB-induced
417 apoptosis was assessed by flow cytometric analysis of subG_1 DNA content. Each point
418 represents the mean +/- SEM determined from three independent experiments. The * and ** in B
419 and C indicate that the value is significantly different from the corresponding non-targeted
420 siRNA transfected control sample ($p<0.05$ and $p<0.01$, respectively), as determined using
421 unpaired t-tests.

A

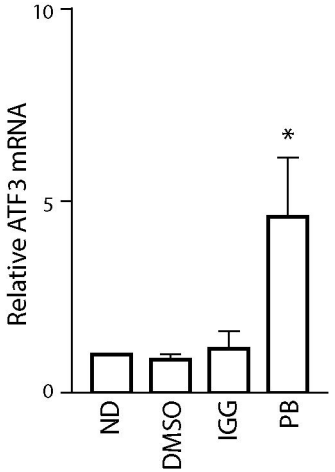
Relative ATF3 mRNA
10
5
0
*
ND
DMSO
IGG
PB

B

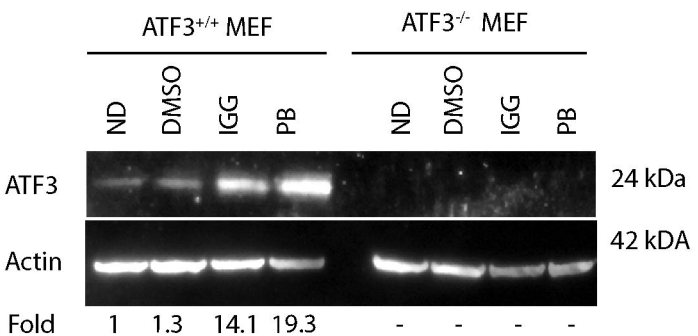
ATF3+/+ MEF
ATF3-/- MEF
ND
DMSO
IGG
PB
ND
DMSO
IGG
PB
ATF3
24 kDa
Actin
42 kDA
Fold
1
1.3
14.1
19.3
-
-
-
-

C

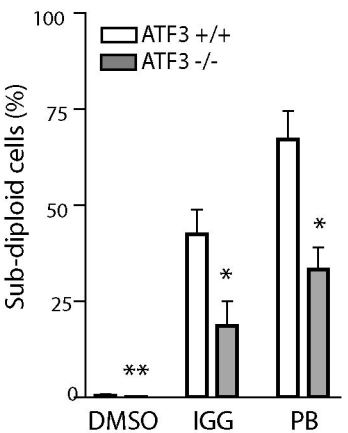
ATF3 +/+
ATF3 -/-
Sub-diploid cells (%)
100
75
50
25
0
**
*
*
DMSO
IGG
PB

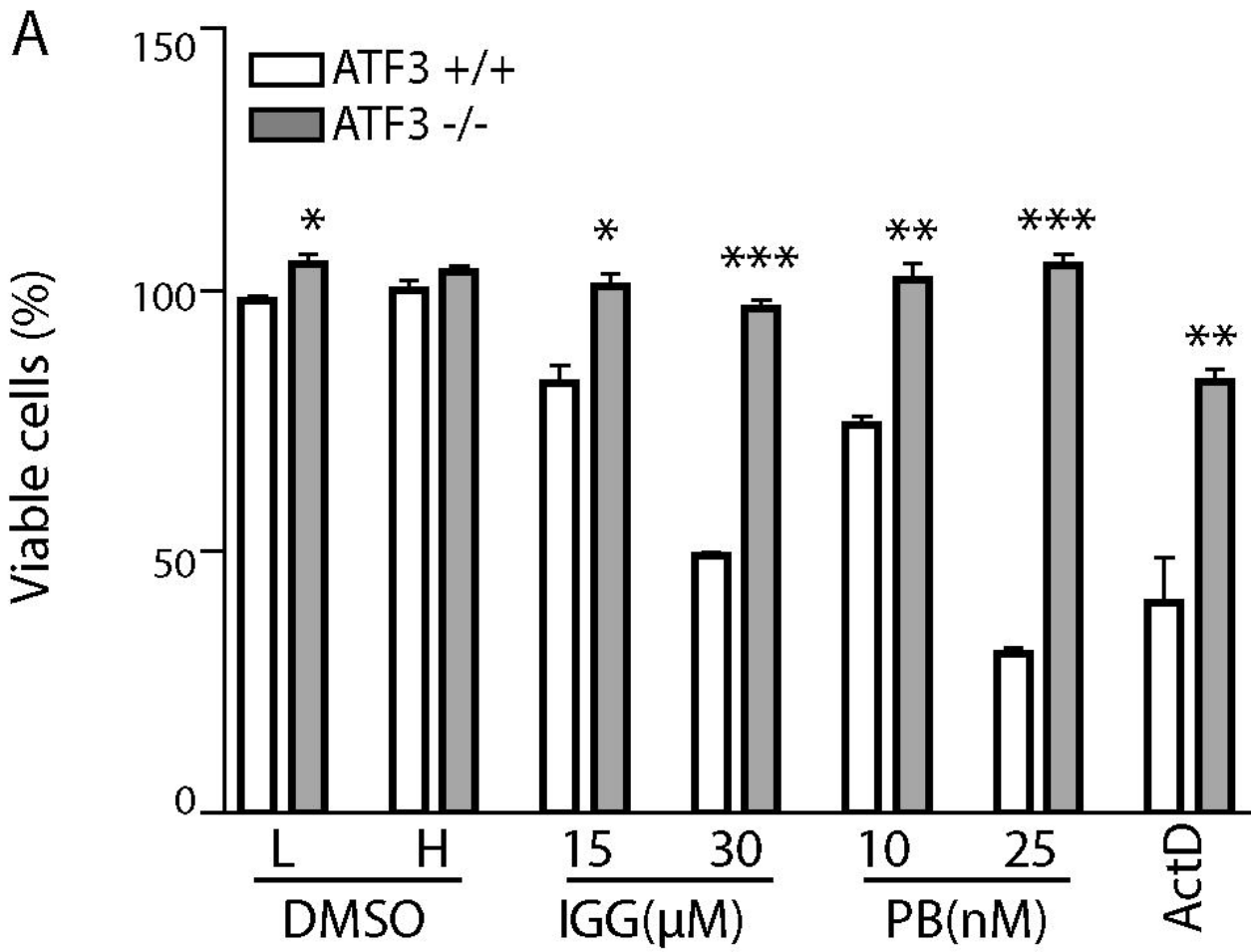
A
ATF3 +/+
ATF3 -/-
Viable cells (%)
150
100
50
0
*
*
***
**
***
**
L
H
15
30
10
25
ActD
DMSO
IGG(μM)
PB(nM)

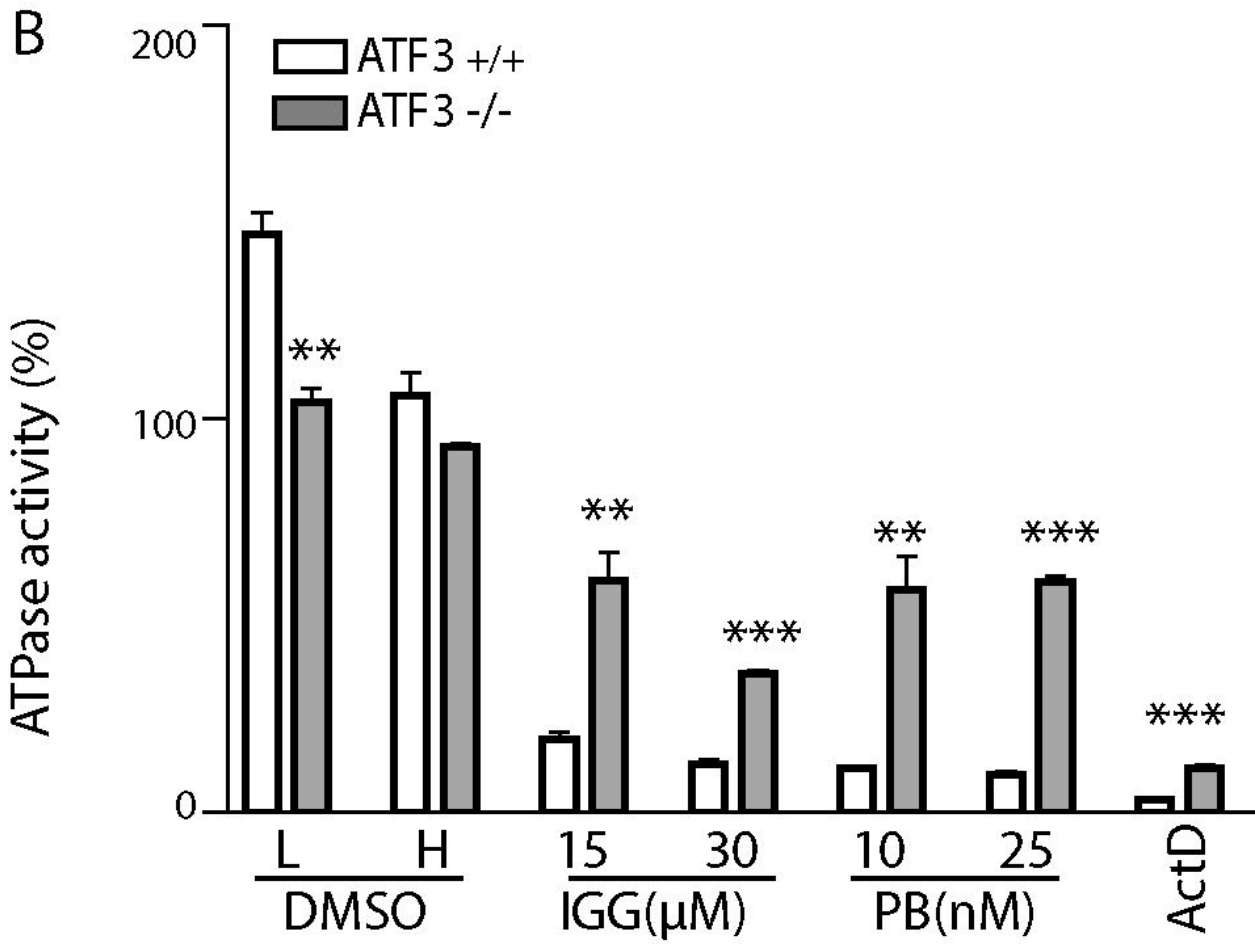
B
ATF3 +/+
ATF3 -/-
ATPase activity (%)
200
100
0
**
**
***
**
***
***
L
H
15
30
10
25
ActD
DMSO
IGG(μM)
PB(nM)

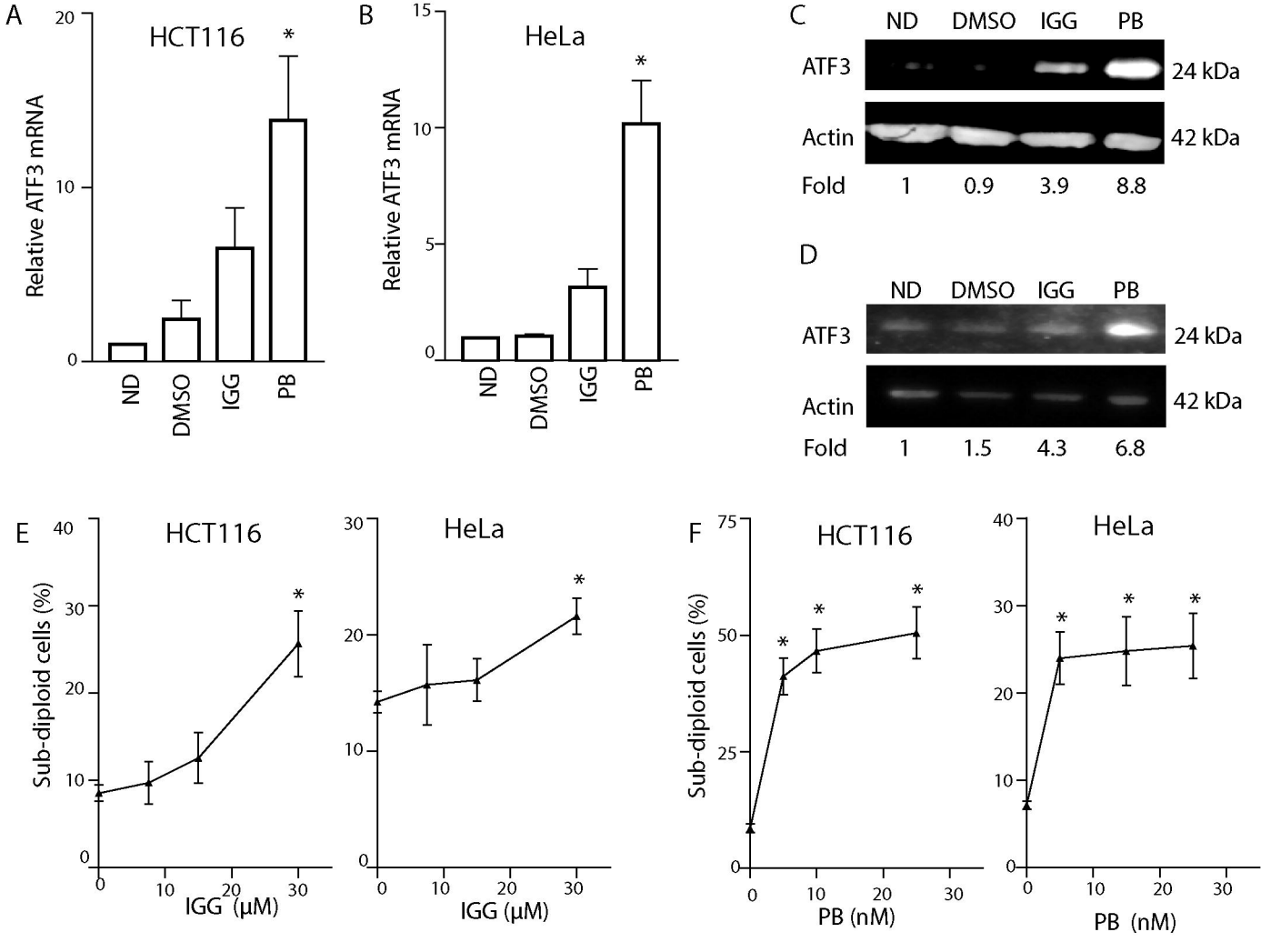
A
HCT116
Relative ATF3 mRNA
20
10
0
*
ND
DMSO
IGG
PB
B
HeLa
Relative ATF3 mRNA
15
10
5
0
*
ND
DMSO
IGG
PB
C
ND
DMSO
IGG
PB
ATF3
24 kDa
Actin
42 kDa
Fold
1
0.9
3.9
8.8
D
ND
DMSO
IGG
PB
ATF3
24 kDa
Actin
42 kDa
Fold
1
1.5
4.3
6.8
E
HCT116
Sub-diploid cells (%)
IGG (μM)
HeLa
IGG (μM)
F
HCT116
Sub-diploid cells (%)
PB (nM)
HeLa
PB (nM)

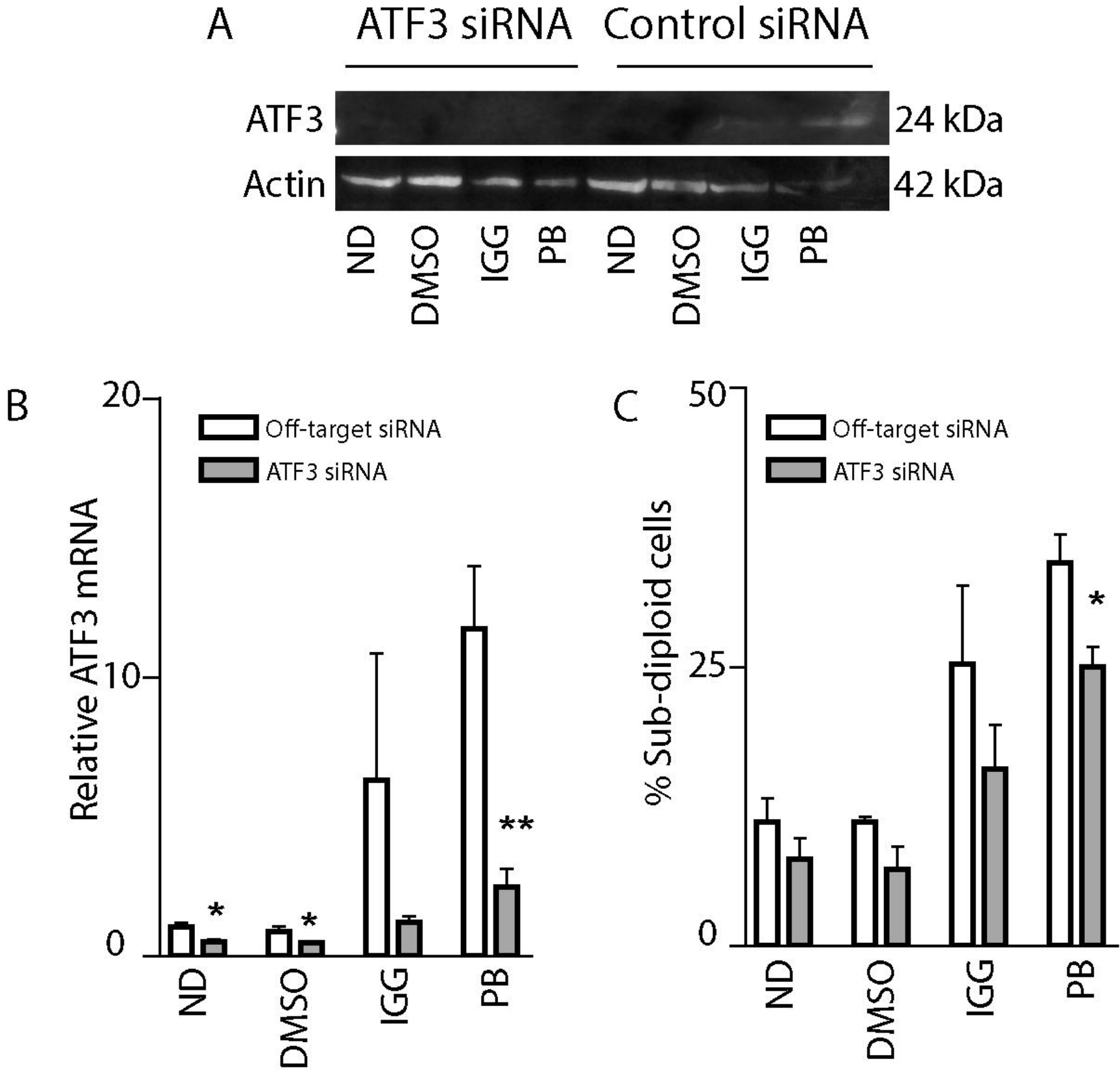
A
ATF3 siRNA
Control siRNA
ATF3
24 kDa
Actin
42 kDa
ND
DMSO
IGG
PB
ND
DMSO
IGG
PB
B
Off-target siRNA
ATF3 siRNA
Relative ATF3 mRNA
20
10
0
*
*
**
ND
DMSO
IGG
PB
C
Off-target siRNA
ATF3 siRNA
% Sub-diploid cells
50
25
0
*
ND
DMSO
IGG
PB